Journal of Hazardous Materials 179 (2010) 244–250

Contents lists available at ScienceDirect

Journal of Hazardous Materials

journal homepage: www.elsevier.com/locate/jhazmat

Adsorption of phosphate from aqueous solution by hydroxy-aluminum, hydroxy-iron and hydroxy-iron–aluminum pillared bentonites

Liang-guo Yan[a], Yuan-yuan Xu[b], Hai-qin Yu[b,c], Xiao-dong Xin[a], Qin Wei[b], Bin Du[a,*]

[a] College of Resources and Environmental Sciences, University of Jinan, Jinan 250022, PR China
[b] College of Chemistry and Chemical Engineering, University of Jinan, Jinan 250022, PR China
[c] College of Chemistry and Chemical Engineering, Ocean University of China, Qingdao 266100, PR China

ARTICLE INFO

Article history:
Received 22 September 2009
Received in revised form 6 January 2010
Accepted 25 February 2010
Available online 3 March 2010

Keywords:
Pillared bentonite
Phosphate
Adsorption isotherm
Adsorption kinetics
Thermodynamics

ABSTRACT

Phosphorus removal is important for the control of eutrophication, and adsorption is an efficient treatment process. In this study, three modified inorganic-bentonites: hydroxy-aluminum pillared bentonite (Al-Bent), hydroxy-iron pillared bentonite (Fe-Bent), and mixed hydroxy-iron–aluminum pillared bentonite (Fe–Al-Bent), were prepared and characterized, and their phosphate adsorption capabilities were evaluated in batch experiments. The results showed a significant increase of interlayer spacing, BET surface area and total pore volume which were all beneficial to phosphate adsorption. Phosphate adsorption capacity followed the order: Al-Bent > Fe-Bent > Fe–Al-Bent. The adsorption rate of phosphate on the adsorbents fits pseudo-second-order kinetic models (R^2 = 1.00, 0.99, 1.00, respectively). The Freundlich and Langmuir models both described the adsorption isotherm data well. Thermodynamic studies illustrated that the adsorption process was endothermic and spontaneous in nature. Finally, phosphate adsorption on the inorganic pillared bentonites significantly raised the pH, indicating an anion/OH^- exchange reaction.

1. Introduction

Phosphorus (P) is an essential nutrient for the growth of organisms in most ecosystems, but superfluous phosphorus can also cause eutrophication and hence deteriorate water quality. Phosphorus is released into aquatic environments in many ways, of which the most significant are human industrial, agricultural, and mining activities. Although phosphorus removal is required before discharging wastewater into bodies of water, phosphorus pollution is nevertheless increasing. Therefore, there is currently an urgent demand for improved phosphorus removal methods which can be applied before wastewater discharge.

Phosphorus removal from wastewater has been widely investigated and several techniques have been developed including adsorption methods, physical processes (settling, filtration), chemical precipitation (with aluminum, iron and calcium salts), and biological processes that rely on biomass growth (bacteria, algae, plants) or intracellular bacterial polyphosphates accumulation [1]. Recently, the removal of phosphate from aqueous solutions via adsorption has attracted much attention. The key problem for many phosphorus adsorption methods, however, is finding an efficient adsorbent. Several low-cost or easily available clays, waste materials and by-products such as zeolite [2], palygorskite [3], fly ash [4], blast furnace slag [5], hydroxides sludge [6], oxide tailings [7], activated aluminum oxide and ferric hydroxide [8], have all been studied extensively and systematically.

Bentonite is a low-cost and easily obtained clay mineral. The high negative charge of bentonite surfaces is usually balanced by alkali metals and alkali earth cations (typically Na^+ and Ca^{2+}). These cations can be replaced by inorganic hydroxyl-metal polycations acting as pillars which increase the interlayer spacing of bentonite. Many different hydroxy-metal polycations including Al [9], Zr [10], Fe [11], Cr [12], Ti [13], Co [14], and Ga [15] have all been used in the past. One of the most intensively studied polycations is hydroxy-aluminum (Keggin ions), the chemical composition and structure of which has been well defined [16]. Various inorganic pillared bentonites have been prepared and employed to remove heavy metals [17], dyes [18], gases [19,20], and other environmental pollutants [21–23].

In contrast to the abundant research dedicated to the adsorption of phosphorus onto many low-cost materials and the preparation of pillared bentonites as adsorbents or catalysts, there are very few studies on the use of pillared bentonites for phosphorus removal from aqueous solutions. Zhu and Zhu [24] synthesized inorganic–organic bentonites (IOBs) by intercalating bentonites with both cetyltrimethyl ammonium bromide (CTMAB) and hydroxy-aluminum to study their simultaneous sorption of organic compounds and phosphate. They found that the phos-

* Corresponding author. Tel.: +86 531 82767370; fax: +86 531 82767370.
E-mail addresses: yanyu-33@163.com (L.-g. Yan), sdjndb@263.com (B. Du).

0304-3894/$ – see front matter © 2010 Elsevier B.V. All rights reserved.
doi:10.1016/j.jhazmat.2010.02.086

phate removal efficiency of IOBs was higher than that of the corresponding hydroxy-aluminum pillared bentonites. Kasama et al. [25] showed that phosphate sorption on Al-pillared smectites was closely related to the OH functional groups of the Al clusters, but only slightly related to the phosphate species in solution. Violante and Gianfreda [26] investigated competitive adsorption between phosphate and oxalate on Al hydroxide montmorillonite complexes.

The objective of this study is to examine the feasibility of using inorganic pillared bentonites as adsorbents for phosphate removal. Three inorganic pillared bentonites, namely hydroxy Al-, Fe- and Fe–Al-pillared bentonites were prepared for use in experiments and their structure and morphology were thoroughly characterized. The phosphate adsorption properties (adsorption kinetics, adsorption isotherms, thermodynamics and pH effect) were also evaluated utilizing batch experimental methods.

2. Materials and methods

2.1. Starting materials

The bentonite used for this study was purchased from the Fangzi bentonite plant (Weifang, Shandong Province, China). NaCl, Na_2CO_3, $Fe(NO_3)_3$, $AlCl_3$, NaOH, and KH_2PO_4 were all of analytical grade, obtained from Sinopharm Chemical Reagent Beijing Co., Ltd, China. All of the reagents were used as received.

2.2. Preparation of adsorbents

2.2.1. Preparation of sodium bentonite

The native bentonite was converted to sodium bentonite (denoted Na-Bent) before the synthesis of inorganic pillared bentonites. First, the natural bentonite was dispersed in deionized water by intense shaking for about 6 h. The <2 μm fraction of the bentonite was collected according to Stokes law. Then the clay was dispersed in 1.0 mol/L NaCl solution and stirred at room temperature for 12 h. The supernatant was removed after settling. This procedure was repeated 3 times. After complete exchange, Na-Bent was separated by centrifugation and washed with deionized water until no chloride was present, confirmed by the $AgNO_3$ test. The solid was dried at 80 °C, ground to 100 mesh, and kept in a sealed bottle.

2.2.2. Preparation of pillaring solutions

The pillaring solution of hydroxy-aluminum oligomeric cations ($[Al_{13}O_4(OH)_{24}H_2O)_{12}]^{7+}$) was prepared by slowly adding 0.48 mol/L NaOH solution to 0.2 mol/L $AlCl_3$ solution under vigorous stirring at 60 °C, until the OH^-/Al^{3+} molar ratio reached 2.4. The solution was stored at 60 °C for 24 h.

To prepare iron pillaring solutions, 0.4 mol/L Na_2CO_3 was slowly added to an aqueous solution of 0.2 mol/L $Fe(NO_3)_3{\cdot}9H_2O$ while mixing vigorously at 60 °C to obtain a OH^-/Fe^{3+} molar ratio of 2.0 [27]. The solution was stored at 60 °C for 24 h.

To prepare pillaring solutions of Fe–Al-Bent, 0.2 mol/L aqueous solution of $AlCl_3{\cdot}6H_2O$ was added to 0.2 mol/L aqueous solution of $Fe(NO_3)_3{\cdot}9H_2O$ at a ratio of $Al^{3+}/Fe^{3+} = 4$ [28], then, 0.2 mol/L Na_2CO_3 was slowly added to the mixing solution to obtain a $OH^-/(Fe^{3+} + Al^{3+})$ molar ratio of 1.2 while mixing vigorously at 60 °C. This pillaring solution was also stored for 24 h at 60 °C.

2.2.3. Preparation of inorganic pillared bentonites

The resulting pillaring solutions were added drop-wise to a 1% (by weight) Na-Bent suspension by stirring for 12 h at the ratio of 10 mmol oligomeric cations per gram of Na-Bent. The slurry was stirred for 24 h at room temperature, filtered, and washed repeatedly with deionized water until there was no chloride, verified by the $AgNO_3$ test. The solid was dried at 80 °C, ground to 100 mesh, and kept in a sealed bottle. The three inorganic pillared bentonites were designated as Al-Bent, Fe-Bent and Fe–Al-Bent respectively.

2.3. Characterization methods

XRD patterns of the prepared samples were acquired with a Rigaku D/MAX 2200 X-ray diffractometer (Tokyo, Japan) using Cu*K*α radiation (40 kV, 300 mA) of wavelength 0.154 nm to confirm the structure of the materials. Surface area measurements were performed on Micromeritics ASAP 2020 surface area and porosity analyzer (Quantachrome, United States). The samples were out-gassed overnight (12 h) under nitrogen prior to adsorption measurement. Pore distributions and pore volume were calculated using the adsorption branch of the N_2 isotherms based on the BJH model. Specific surface area was calculated on the basis of the BET equation. Pillared bentonite samples were coated with Au under vacuum in an argon atmosphere for scanning electron microscopy (SEM) (Hitachi S570, Tokyo, Japan).

2.4. General batch adsorption procedure

For the adsorption of phosphate, phosphate stock solution of 100 mg/L (calculated as P, hereafter) was prepared by dissolving KH_2PO_4 in deionized water, and dilutions of the stock solution were used in subsequent experiments. In the isotherm experiments, 0.1 g of inorganic pillared bentonite (Al-Bent, Fe-Bent and Fe–Al-Bent) and 25 mL of 25–60 mg/L P solution were mixed in a series of Teflon centrifuge tubes. The pH was adjusted to 3.0 by adding a few drops of 1 mol/L HCl or 1 mol/L NaOH solution. The tubes were capped and placed on an orbital shaker at 170 rpm for 6 h to ensure equilibrium. The suspension was separated by centrifugation (8000 *r*/min, 10 min) and the supernatant was filtered through a 0.45 μm membrane filter. The residual concentration of phosphate was determined by the molybdate blue spectrophotometric method. Each experiment was duplicated under identical conditions.

Blank samples (containing only deionized water and corresponding inorganic pillared bentonites) were prepared and monitored for the duration of the experiment as a control.

3. Results and discussion

3.1. Characterization

X-ray diffraction patterns of the samples are illustrated in Fig. 1. Natural clay had typical X-ray diffractograms of bentonite (Fig. 1E). The main compensating cations were calcium and magnesium, which was in agreement with the observed d_{001} distance of 1.46 nm. The d_{001} value decreased to 1.24 nm when Ca^{2+} and Mg^{2+} ions were fully exchanged by Na^+ ions for their lower radii in the layer of bentonite. After hydroxy-aluminum and hydroxy-iron–aluminum polycations exchange, the d_{001} value increased to 1.88 and 1.76 nm, respectively (Table 1). The d_{001} result of Al-Bent is in accordance with that of Zhu and Zhu [24], who reported that the 1.9 nm basal spacing for the Al-Bent consisted of a 1.0 nm height of clay layers and 0.9 nm height of Al_{13} polycations. Comparing basal spacings among the Al-Bent, Fe–Al-Bent and Na-Bent samples, the increase in interlayer spacing indicated that the hydroxy-aluminum and hydroxy-iron–aluminum polycations had been intercalated into the interlayer of Na-Bent. However, the d_{001} value of Fe-Bent cannot be observed because the Fe oligomers between clay layers have changed the typical X-ray diffraction patterns. The (0 0 1) peaks of Fe–Al-Bent and Fe-Bent were much less intense compared to those of Na-Bent and Al-Bent in agreement with previous results obtained by Zhu et al. [29].

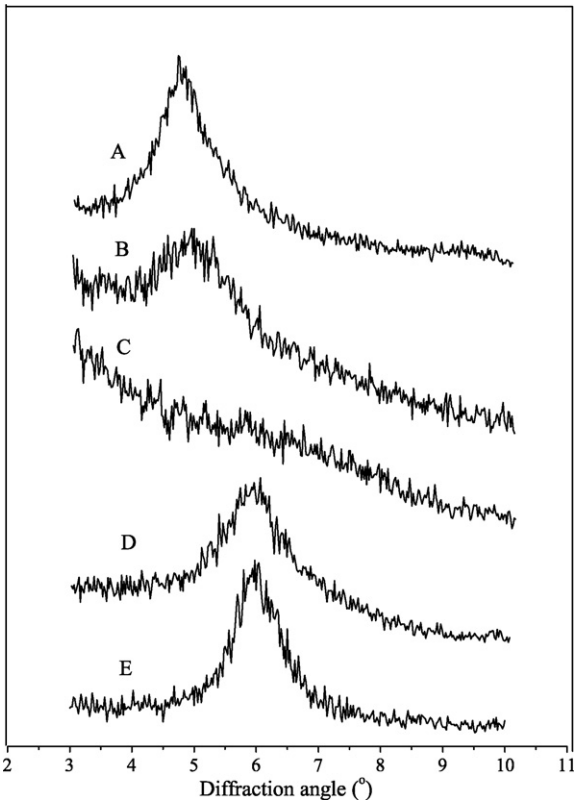

Fig. 1. XRD patterns of (A) Al-Bent, (B) Fe–Al-Bent, (C) Fe-Bent, (D) Na-Bent amd (E) natural bentonite.

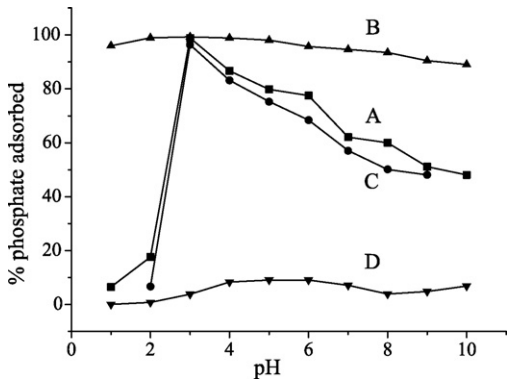

Fig. 2. Effect of initial pH on phosphate adsorption onto (A) Al-Bent, (B) Fe-Bent and (C) Fe–Al-Bent, (D) Na-Bent. Phosphate concentration 20 mg/L, contact time 6 h, adsorbent dose 4 g/L.

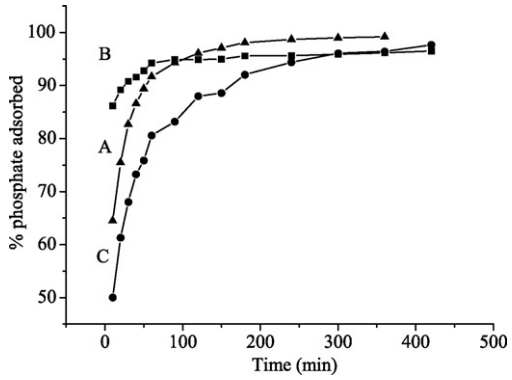

Fig. 3. Effect of contact time on phosphate adsorption onto (A) Al-Bent, (B) Fe-Bent and (C) Fe–Al-Bent. Phosphate concentration 20 mg/L, initial pH 3, adsorbent dose 4 g/L.

Table 1 shows the BET surface area and total pore volume for the different samples. The BET surface area of Al-Bent was far larger than that of Fe-Bent and Fe–Al-Bent which may result from a high phosphate adsorption capacity.

3.2. Effect of initial pH on phosphate adsorption

The amount of phosphate adsorbed onto Na-Bent and inorganic pillared bentonites at various pH values is illustrated in Fig. 2. Phosphate was hardly adsorbed by Na-Bent (Fig. 2D), so Na-Bent is not discussed further. For the other three inorganic pillared bentonites, phosphorus adsorption appears to peak at pH 3.

As presented in Fig. 2, pH exerts a significant impact on phosphate adsorption for both Al-Bent and Fe–Al-Bent. The amount of phosphate adsorbed increased below pH 3 and decreased above pH 3. The optimal pH for phosphate adsorption ranged between 3 and 5, at which point the dominant phosphate form is the monovalent $H_2PO_4^-$ ion. The adsorption is possibly favored by low pH values because of anion adsorption coupling with the release of hydroxyl anions [30]. The decrease in phosphate adsorption after pH 3 could be due to a change in surface charge caused by the inorganic pillared bentonites becoming more negative at higher pH values. This process would then strengthen the electrostatic repulsion between the exchange site and the incoming phosphate ions [31,32].

Phosphate adsorption by Fe-Bent, however, appeared to be less pH-dependent. Compared to the maximum amount of adsorbed phosphate for Fe-Bent, less than a 10% decrease in phosphate adsorption was observed across a wide range of pH values. The presence of the iron polycations in the interlayer of bentonite most likely enhanced the affinity of the microporous interlayer sites towards the phosphate [7].

3.3. Adsorption kinetics

The adsorption of phosphate on the three adsorbents increased with time and reached equilibrium at about 6 h (Fig. 3). The adsorption kinetics data of phosphate were determined by testing pseudo-first order and pseudo-second-order kinetic models. Better agreement was achieved for the pseudo-second-order equation [33]:

$$\frac{dq_t}{dt} = k(q_e - q_t)^2 \quad (1)$$

where q_t (mg/g) is the adsorbed amount at time t, k (mg/(g min)) is the equilibrium rate constant of the pseudo-second-order kinetics model and q_e (mg/g) is the adsorbed amount at equilibrium. Inte-

Table 1
Summary of XRD and BET analysis results of Na-Bent, Al-Bent, Fe-Bent and Fe–Al-Bent.

Adsorbent	BET surface area (m^2/g)	Total pore volume (cm^3/g)	Average pore diameter (nm)	d_{001} (nm)
Na-Bent	31.7	0.0608	7.67	1.24
Al-Bent	200	0.152	3.03	1.88
Fe-Bent	143	0.211	5.91	–
Fe–Al-Bent	94.9	0.0973	4.10	1.76

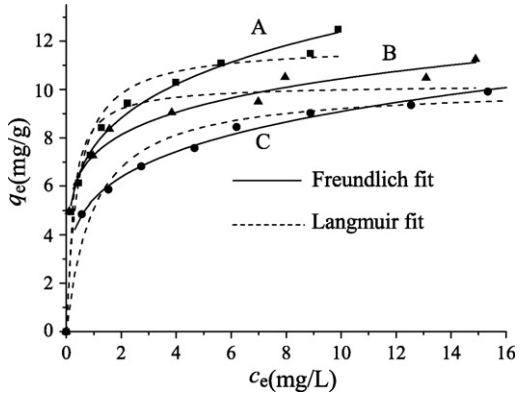

Fig. 4. The adsorption isotherms of phosphate by (A) Al-Bent, (B) Fe-Bent and (C) Fe–Al-Bent at room temperature. Adsorbent dose 4 g/L, initial pH 3, contact time 6 h, initial phosphate concentration 25–60 mg/L.

grating Eq. (1) for the boundary condition $t = 0$ to $t = t$ and $q_t = 0$ to $q_t = q_t$, it was rearranged to obtain a linear form:

$$\frac{t}{q_t} = \frac{1}{kq_e{}^2} + \frac{1}{q_e}t \quad (2)$$

A plot of t/q_t against t should give a linear relationship with a slope of $1/q_e$ and an intercept of $1/kq_e{}^2$. The constants k and q_e were calculated from the linear plot of t/q_t vs. t. The good agreement of the data with the pseudo-second-order kinetics model ($R^2 = 1.00$, 0.99, 1.00, respectively) suggested that the chemisorption process could be a rate-limiting step [33]. The values of q_e for Al-Bent, Fe-Bent and Fe–Al-Bent were 5.05, 4.84, and 4.64 mg/g respectively, indicating an Al-Bent > Fe-Bent > Fe–Al-Bent order for phosphate adsorption capacity.

3.4. Adsorption isotherms

The adsorption isotherms of phosphate on the three inorganic pillared bentonites were studied using the optimized conditions: adsorbent dose 4 g/L, initial pH 3, contact time 6 h, and the results are shown in Fig. 4. The Langmuir and Freundlich equations expressed in Eqs. (3) and (4) were used for modeling these adsorption isotherm data.

$$q_e = \frac{bq_m c_e}{1 + bc_e} \quad (3)$$

$$q_e = K_f c_e{}^{1/n} \quad (4)$$

where c_e (mg/L) and q_e (mg/g) are the equilibrium adsorbate concentrations in the aqueous and solid phases. Here, q_m (mg/g) is the maximum adsorption capacity and b is the Langmuir adsorption equilibrium constant. K_f is the Freundlich equilibrium constant indicative of adsorption capacity and $1/n$ is the Freundlich adsorption constant, the reciprocal of which is indicative of adsorption intensity.

The fitted constants for the Langmuir and Freundlich isotherm models along with regression coefficients (R^2) are summarized in Table 2. The R^2 values obtained for the Freundlich and Langmuir isotherms were both above 0.98, indicating a very good mathematical fit by both models. Similar results have been reported for the adsorption of phosphate by akaganéite and hybrid surfactant-akaganéite [34], and alkaline fly ash [35].

From Table 2, the calculated q_m and K_f followed the order of Al-Bent > Fe-Bent > Fe–Al-Bent which indicate the capacity of phosphate adsorption. The result is in agreement with the above-mentioned conclusion obtained from adsorption kinetics. All the isotherms showed a similar shape and were nonlinear over a wide range of aqueous equilibrium concentrations in Fig. 4.

Table 2
Freundlich and Langmuir constants and regression coefficients for adsorption of phosphate onto inorganic pillared bentonites.

Model	Parameter	Al-Bent	Fe-Bent	Fe–Al-Bent
Freundlich equation	K_f	7.56	7.43	5.54
	$1/n$	0.216	0.161	0.213
	R^2	0.984	0.981	0.996
Langmuir equation	q_m (mg/g)	12.7	11.2	10.5
	b (L/mg)	1.61	1.83	1.25
	R^2	0.994	0.995	0.990

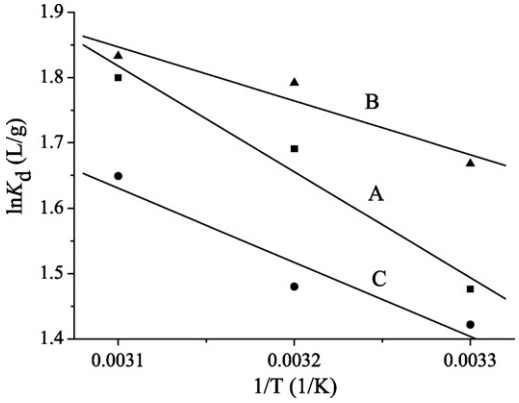

Fig. 5. Plots of $\ln K_d$ vs. $1/T$ for (A) Al-Bent, (B) Fe-Bent and (C) Fe–Al-Bent. Adsorbent dose 4 g/L, initial pH 3, contact time 6 h, initial phosphate concentration 25–60 mg/L.

3.5. Adsorption thermodynamics

The influence of temperature on phosphate adsorption onto inorganic pillared bentonites was carried out at temperatures ranging from 303 to 323 K with an initial phosphate concentration between 25 and 60 mg/L, pH 3, and a fixed adsorbent dose of 4 g/L.

The thermodynamic equilibrium constants (K_d) of the adsorption process, i.e. the constants for phosphate distribution between the solid and liquid phases at equilibrium, were computed using the method of Lyubchik et al. [36] by plotting $\ln(q_e/C_e)$ versus q_e and extrapolating q_e to zero. The change in Gibbs free energies (ΔG) was then calculated with Eq. (5). ΔH and ΔS were calculated from the slope and intercept of the plot of $\ln K_d$ versus $1/T$ using Eq. (6) which is shown in Fig. 5.

$$\Delta G = -RT \ln K_d \quad (5)$$

$$\ln K_d = \frac{\Delta S}{R} - \frac{\Delta H}{RT} \quad (6)$$

All the thermodynamic parameters are listed in Table 3. The negative values of ΔG and positive values of ΔH indicate that the adsorption of phosphate onto Al-Bent, Fe-Bent and Fe–Al-Bent is spontaneous and endothermic. The values of ΔG decreased from

Table 3
Thermodynamic data for adsorption of phosphate onto Al-Bent, Fe-Bent and Fe–Al-Bent.

Adsorbent	T (K)	K_d (L/g)	ΔG (kJ/mol)	ΔS (J/mol)	ΔH (kJ/mol)
Al-Bent	303	4.38	−3.72	56.9	13.5
	313	5.43	−4.40		
	323	6.05	−4.83		
Fe-Bent	303	5.30	−4.20	36.6	6.86
	313	6.00	−4.66		
	323	6.25	−4.92		
Fe–Al-Bent	303	4.15	−3.58	42.8	9.44
	313	4.39	−3.85		
	323	5.20	−4.43		

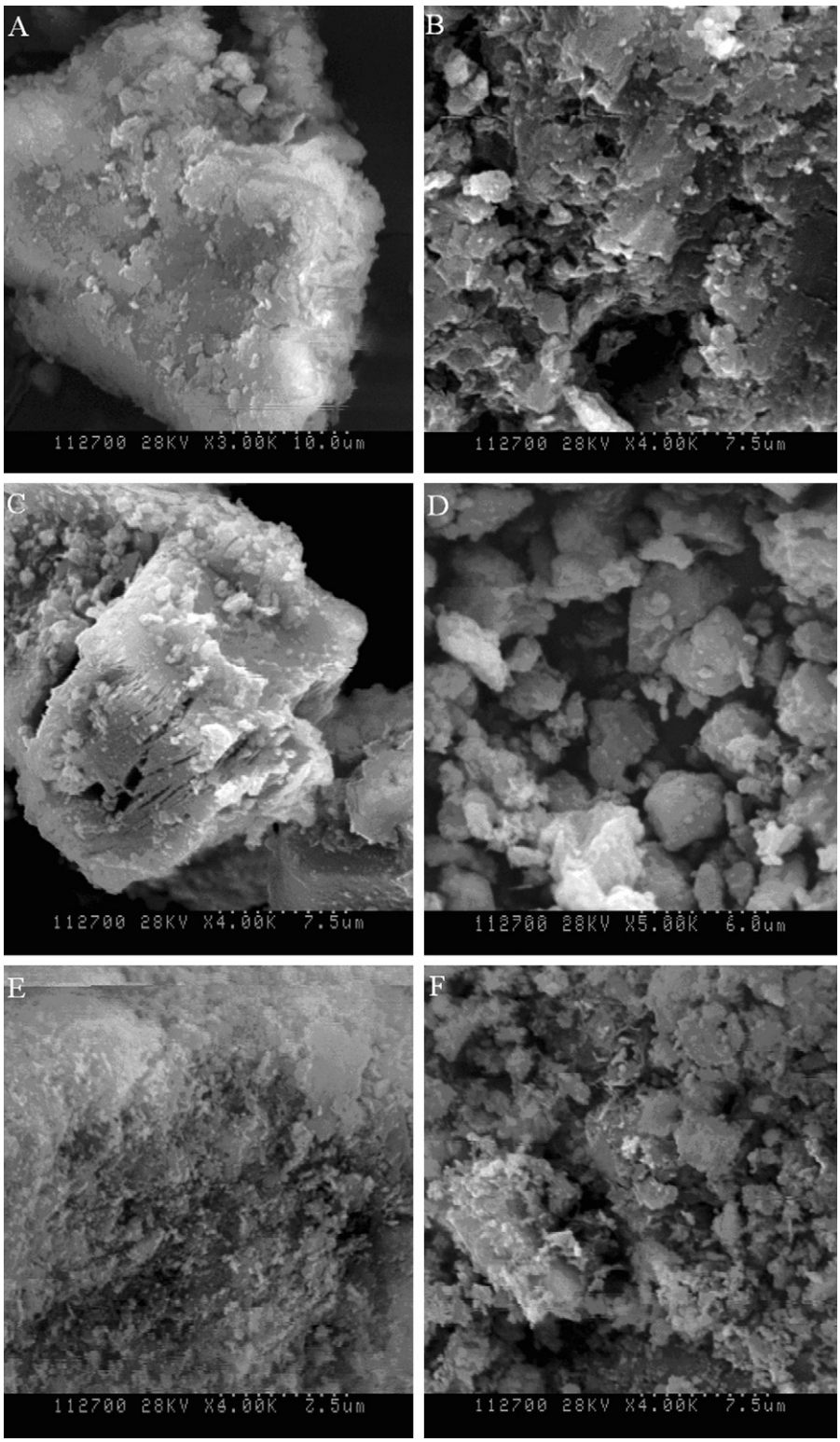

Fig. 6. SEM images of (A and B) Al-Bent, (C and D) Fe-Bent and (E and F) Fe–Al-Bent before (A, C and E) and after (B, D and F) phosphate adsorption.

−3.72 to −4.83 kJ/mol (Al-Bent), −4.20 to −4.92 kJ/mol (Fe-Bent), −3.58 to −4.43 kJ/mol (Fe–Al-Bent) in the temperature range of 303–323 K. The endothermic adsorption of phosphate onto the pillared bentonites was enhanced by an increase in temperature. The values of ΔH are high enough to ensure strong interaction between the phosphate and the adsorbents. The positive values of ΔS state clearly that the randomness increased at the solid–solution interface during the phosphate adsorption onto the inorganic pillared bentonites. The increase in adsorption capacity of pillared bentonites at higher temperatures may be caused by the enlargement of pore size and/or activation of the adsorbent surface [37].

3.6. Adsorption mechanisms

It is well known that certain anions (phosphate, nitrate, arsenate, etc.) are adsorbed onto clays via electrostatic attraction and

ligand exchange [32,38,39]. This process of ligand exchange can change the pH value of the adsorption system [24]. In this study, the pH values of all the phosphate–bentonite solutions increased from about 3.0 to 3.9–4.3 for the Al-Bent system, 5.1–6.1 for the Fe-Bent system, and 4.0–4.4 for the Fe–Al-Bent system, indicating a ligand exchange process occurred during adsorption. The presence of the Al–OH and Fe–OH functional groups contributed to the adsorption. At low pH, surface hydroxyl groups are protonized, and facilitate in the ligand exchange process because $-OH_2^+$ is easier to displace from the metal binding sites than hydroxyl groups [40]. On the inorganic pillared bentonites, phosphate replaced the hydroxyl groups, which were then released into the solution. Previous results from phosphate adsorption kinetics experiments agreeing with the pseudo-second-order equation suggested a chemisorption process. The attachment of phosphate must occur at the active sites on the surface of the pillared bentonites. Therefore, the adsorption of phosphate species can be reasonably speculated to occur in two steps: (1) transfer of phosphate from the aqueous solution to the sites on the adsorbent; (2) chemical complexation/ion exchange at the active sites [31,41,42].

SEM images of the raw and treated adsorbents were used to examine the pillared clay surface before and after phosphate adsorption (Fig. 6). Significant differences were observed between the micrographs of the raw adsorbent surfaces taken before and after phosphate adsorption. Al-Bent, Fe-Bent and Fe–Al-Bent exhibited an aggregated morphology and several large flakes were observed in some instances. After phosphate adsorption, a number of thin lamellas formed a stacking structure decreased the size of the intra-particle voids. This indicated that phosphate did adsorb onto the surface, fundamentally changing the character of the pillared bentonites by compacting the crystal lattice [5,43].

4. Conclusions

In this study, three prepared inorganic-bentonites were applied to remove phosphate ions from aqueous solution. The adsorption isotherms, kinetics, pH effect, equilibrium time and thermodynamics were also examined. Structural characterization shows that the combined effects of interlayer spacing, BET surface area and total pore volume allow for the removal of more than 80% of the phosphate from water within 1 h. The pseudo-second-order model accurately described the phosphate adsorption kinetics for the three prepared inorganic-bentonites and the data agrees well with both the Freundlich and Langmuir adsorption isotherm models. Thermodynamic studies showed that the adsorption process was endothermic and spontaneous in nature. Aqueous phosphate solutions with a wide range of concentrations were adsorbed by inorganic pillared bentonites. The final adsorption efficiency was higher than 90%, suggesting that these structures are excellent adsorbents for effective phosphate removal from water.

Acknowledgments

This study was supported by the Natural Science Foundation of China (20577016), Department of Science & Technology of Shandong Province (2008BS09008), and Project of Shandong Province Higher Educational Science and Technology Program (J08LC06). Thanks to Chris P. Tostado at Tsinghua University and Dr. Edward C. Mignot at Shandong University for their suggestions and advice.

References

[1] L.E. de-Bashana, Y. Bashan, Recent advances in removing phosphorus from wastewater and its future use as fertilizer (1997–2003), Water Res. 38 (2004) 4222–4246.
[2] D. Wu, B. Zhang, C. Li, Z. Zhang, H. Kong, Simultaneous removal of ammonium and phosphate by zeolite synthesized from fly ash as influenced by salt treatment, J. Colloid Interface Sci. 304 (2006) 300–306.
[3] H. Ye, F. Chen, Y. Sheng, G. Sheng, J. Fu, Adsorption of phosphate from aqueous solution onto modified palygorskites, Sep. Purif. Technol. 50 (2006) 283–290.
[4] J. Chen, H. Kong, D. Wu, X. Chen, D. Zhang, Z. Sun, Phosphate immobilization from aqueous solution by fly ashes in relation to their composition, J. Hazard. Mater. 139 (2007) 293–300.
[5] E. Oguz, Removal of phosphate from aqueous solution with blast furnace slag, J. Hazard. Mater. 114 (2004) 131–137.
[6] A.K. Golder, A.N. Samanta, S. Ray, Removal of phosphate from aqueous solutions using calcined metal hydroxides sludge waste generated from electrocoagulation, Sep. Purif. Technol. 52 (2006) 102–109.
[7] L. Zeng, X. Li, J. Liu, Adsorptive removal of phosphate from aqueous solutions using iron oxide tailings, Water Res. 38 (2004) 1318–1326.
[8] A. Genz, A. Kornmüller, M. Jekel, Advanced phosphorus removal from membrane filtrates by adsorption on activated aluminium oxide and granulated ferric hydroxide, Water Res. 38 (2004) 3523–3530.
[9] G.R. Rao, B.G. Mishra, A comparative UV-vis-diffuse reflectance study on the location and interaction of cerium ions in Al- and Zr-pillared montmorillonite clays, Mater. Chem. Phys. 89 (2005) 110–115.
[10] B.G. Mishra, G.R. Rao, Physicochemical and catalytic properties of Zr-pillared montmorillonite with varying pillar density, Micropor. Mesopor. Mater. 70 (2004) 43–50.
[11] M.D. Bhor, N.S. Nandurkar, M.J. Bhanushali, Ultrasound promoted selective synthesis of 1,1′-binaphthyls catalyzed by Fe impregnated pillared montmorillonite K10 in presence of TBHP as an oxidant, Ultrason. Sonochem. 15 (2008) 195–202.
[12] M. Roulia, Synthesis and characterization of novel chromium pillared clays, Mater. Chem. Phys. 91 (2005) 281–288.
[13] C. Ooka, H. Yoshida, M. Horio, K. Suzuki, T. Hattori, Adsorptive and photocatalytic performance of TiO_2 pillared montmorillonite in degradation of endocrine disruptors having different hydrophobicity, Appl. Catal. B 41 (2003) 313–321.
[14] A. Ezabadi, G.R. Najafi, M.M. Hashemi, A green and efficient deoximation using H_2O_2 catalyzed by montmorillonite-K10 supported $CoCl_2$, Chin. Chem. Lett. 18 (2007) 1451–1454.
[15] L. Duong, T. Bostrom, T. Kloprogge, R. Frost, The distribution of Ga in Ga-pillared montmorillonites: a transmission electron microscopy and microanalysis study, Micropor. Mesopor. Mater. 82 (2005) 165–172.
[16] P. Salerno, S. Mendioroz, Preparation of Al-pillared montmorillonite from concentrated dispersions, Appl. Clay Sci. 22 (2002) 115–123.
[17] D. Karamanis, P.A. Assimakopoulos, Efficiency of aluminum-pillared montmorillonite on the removal of cesium and copper from aqueous solutions, Water Res. 41 (2007) 1897–1906.
[18] Z. Bouberka, A. Khenifi, N. Benderdouche, Z. Derriche, Removal of Supranol Yellow 4GL by adsorption onto Cr-intercalated montmorillonite, J. Hazard. Mater. 133 (2006) 154–161.
[19] A. Itadani, M. Tanaka, T. Abe, H. Taguchi, M. Nagao, Al-pillared montmorillonite clay minerals: low-pressure CO adsorption at room temperature, J. Colloid Interface Sci. 313 (2007) 747–750.
[20] D. Nguyen-Thanh, K. Block, T.J. Bandosz, Adsorption of hydrogen sulfide on montmorillonites modified with iron, Chemosphere 59 (2005) 343–353.
[21] L. Zhu, J. Ma, Simultaneous removal of acid dye and cationic surfactant from water by bentonite in one-step process, Chem. Eng. J. 139 (2008) 503–509.
[22] B. Chen, W. Huang, Effect of background electrolytes on the adsorption of nitroaromatic compounds onto bentonite, J. Environ. Sci. 21 (2009) 1044–1052.
[23] R. Zhu, L. Zhu, J. Zhu, J. Zhu, F. Ge, T. Wang, Sorption of naphthalene and phosphate to the CTMAB-Al_{13} intercalated bentonites, J. Hazard. Mater. 168 (2009) 1590–1594.
[24] L. Zhu, R. Zhu, Simultaneous sorption of organic compounds and phosphate to inorganic–organic bentonites from water, Sep. Purif. Technol. 54 (2007) 71–76.
[25] T. Kasama, Y. Watanabe, H. Yamada, T. Murakami, Sorption of phosphates on Al-pillared smectites and mica at acidic to neutral pH, Appl. Clay Sci. 25 (2004) 167–177.
[26] A. Violante, L. Gianfreda, Competition in adsorption between phosphate and oxalate on an aluminum hydroxide montmorillonite complex, Soil Sci. Soc. Am. J. 57 (1993) 1235–1241.
[27] T. Mandalia, M. Crespin, D. Messad, F. Bergaya, Large interlayer repeat distances observed for montmorillonites treated by mixed Al–Fe and Fe pillaring solutions, Chem. Commun. 19 (1998) 2111–2112.
[28] J. Guo, A.-D. Muthanna, Catalytic wet oxidation of phenol by hydrogen peroxide over pillared clay catalyst, Ind. Eng. Chem. Res. 42 (2003) 2450–2460.
[29] M.-X. Zhu, K.-Y. Ding, S.-H. Xu, X. Jiang, Adsorption of phosphate on hydroxyaluminum- and hydroxyiron-montmorillonite complexes, J. Hazard. Mater. 165 (2009) 645–651.
[30] P. Ning, H.-J. Bark, B. Li, X. Lu, Y. Zhang, Phosphate removal from wastewater by model-La(III) zeolite adsorbents, J. Environ. Sci. 20 (2008) 670–674.
[31] J. Ma, L. Zhu, Simultaneous sorption of phosphate and phenanthrene to inorgano -organo-bentonite from water, J. Hazard. Mater. 136 (2006) 982–988.
[32] R. Chitrakar, S. Tezuka, A. Sonoda, K. Sakane, K. Ooi, T. Hirotsu, Phosphate adsorption on synthetic goethite and akaganeite, J. Colloid Interface Sci. 298 (2006) 602–608.
[33] Y.-S. Ho, Review of second-order models for adsorption systems, J. Hazard. Mater. 136 (2006) 681–689.

[34] E.A. Deliyanni, E.N. Peleka, N.K. Lazaridis, Comparative study of phosphates removal from aqueous solutions by nanocrystalline akaganéite and hybrid surfactant-akaganéite, Sep. Purif. Technol. 52 (2007) 478–486.
[35] K.C. Cheung, T.H. Venkitachalam, Improving phosphate removal of sand infiltration system using alkaline fly ash, Chemosphere 41 (2000) 243–249.
[36] S.I. Lyubchik, A.I. Lyubchik, O.L. Galushko, L.P. Tikhonova, J. Vital, I.M. Fonseca, S.B. Lyubchik, Kinetics and thermodynamics of the Cr(III) adsorption on the activated carbon from co-mingled wastes, Colloids Surf. A 242 (2004) 151–158.
[37] Y. Masue, R.H. Loeppert, T.A. Kramer, Arsenate arsenite adsorption and desorption behavior on coprecipitated aluminium: iron hydroxides, Environ. Sci. Technol. 41 (2007) 837–842.
[38] Y. Xue, H. Hou, S. Zhu, Characteristics and mechanisms of phosphate adsorption onto basic oxygen furnace slag, J. Hazard. Mater. 162 (2009) 973–980.
[39] Y. Yang, Y.Q. Zhao, A.O. Babatunde, L. Wang, Y.X. Ren, Y. Han, Characteristics and mechanisms of phosphate adsorption on dewatered alum sludge, Sep. Purif. Technol. 51 (2006) 193–200.
[40] M.B. McBride, Environmental Chemistry of Soils, first ed., Oxford University Press, New York, 1994.
[41] Y. Arai, D.L. Sparks, ATR-FTIR spectroscopic investigation on phosphate adsorption mechanisms at the ferrihydrite–water interface, J. Colloid Interface Sci. 241 (2001) 317–326.
[42] J. Antelo, M. Avena, S. Fiol, R. López, F. Arce, Effects of pH and ionic strength on the adsorption of phosphate and arsenate at the goethite–water interface, J. Colloid Interface Sci. 285 (2005) 476–486.
[43] J. Yang, S. Wang, Z. Lu, J. Yang, S. Lou, Converter slag-coal cinder columns for the removal of phosphorus and other pollutants, J. Hazard. Mater. 168 (2009) 331–337.